

Photovoltaic Current Response of Mesoscopic Conductors to Quantized Cavity Modes

Maxim G. Vavilov* and A. Douglas Stone

Department of Applied Physics, Yale University, New Haven, Connecticut 06520, USA

(Received 21 June 2006; published 20 November 2006)

We extend the analysis of the effects of electromagnetic (EM) fields on mesoscopic conductors to include the effects of field quantization, motivated by recent experiments on circuit QED. We show that in general there is a photovoltaic (PV) current induced by quantized cavity modes at zero bias across the conductor. This current depends on the average photon occupation number and vanishes identically when it is equal to the average number of thermal electron-hole pairs. We analyze in detail the case of a chaotic quantum dot at temperature T_e in contact with a thermal EM field at temperature T_f , calculating the rms size of the PV current as a function of the temperature difference, finding an effect \sim pA.

DOI: [10.1103/PhysRevLett.97.216801](https://doi.org/10.1103/PhysRevLett.97.216801)

PACS numbers: 73.23.-b, 72.15.Eb, 73.63.Kv

Many quantum electronic devices for applications in metrology and quantum information technology involve the interaction of electrons with high frequency electromagnetic (EM) fields, often the quantum devices act as detectors of this radiation [1]. In phase-coherent (mesoscopic) devices there are quantum interference effects in electron transport such as the weak localization correction to the conductance and universal conductance fluctuations which can in principle be used to detect radiation since it suppresses these effects [2–4]. In practice the suppression of coherent transport by EM fields is difficult to separate from the suppression by intrinsic interactions due to the electron-electron and electron-phonon couplings.

A more reliable means of using mesoscopic conductors to detect EM radiation is to look at the dc current induced by such a field at zero voltage and temperature bias across the device, known as the mesoscopic photovoltaic (PV) effect [5–8]. This effect arises in mesoscopic conductors because the phase-coherent transmission through the device almost always violates parity symmetry and the non-equilibrium distribution created by the EM field sets up a steady-state current dictated by this parity violation. When the parity violation is due to random interference, the sign of this current will fluctuate from sample to sample and its root-mean-square (rms) size in this case depends on the power in the EM field [5,6,8–11]. Hence this PV current can be used for detection of incident EM fields.

The previous theoretical description [5,6,9–12] of the PV current has employed a classical treatment of the EM fields, since this description was sufficient for the systems studied experimentally [7,8,13–15]. In this case the rms PV current is a monotonically increasing function of the EM field power. Recently a new generation of electronic circuits was developed [16], where a quantum electronic device is coupled to an EM field of a high quality electromagnetic resonator. If the resonator contains a small number of photons of the EM field and the lifetime of the photons is long, the interaction of the EM field with electrons requires a full quantum treatment, based on the

laws of quantum electrodynamics, leading to a new sub-field of quantum electronics known as circuit QED.

In this Letter we investigate the properties of the mesoscopic PV current that arises due to the electron interaction with quantized EM fields. We find that the net current through the device can be represented as the sum of two opposite contributions. One contribution is determined by the average number \bar{N}_i of photons with energy ω_i in modes i of the resonator. The second contribution is determined by the number of thermal electron-hole pairs with energy ω_i of resonator modes i , given by the Bose distribution function $N_B(\omega_i/T_e)$ at temperature T_e of electrons in the leads; $N_B(x) = 1/(e^{x\hbar} - 1)$. We demonstrate that if both contributions are taken into account, the magnitude of the PV current, unlike the classical case, is not a monotonic function of the strength of the EM field. Instead special conditions can be met when these two contributions cancel each other and the PV current vanishes for *all* mesoscopic realizations of the device. For the case of a thermal photon field the zero current state occurs when the temperature of the EM field and that of the electrons in the leads are the same and follows from the principle of detailed balance. For an externally driven single-mode cavity the zero current state also occurs whenever the average number of photons \bar{N}_i is equal to the occupation number of bosons $N_B(\omega_i/T_e)$ at the electron temperature T_e , independent of the other properties of the full photon distribution in the cavity. In the classical description of EM fields only the first contribution is found and the second contribution due to electron-hole pairs is missed. As noted, in this case the PV current never vanishes simultaneously for *all* realizations and its rms value is a monotonic function of the power of the EM radiation [5,6,11,17]. The nonmonotonic behavior of the rms value of the PV current is an indication of the quantum behavior of the EM fields.

A schematic depiction of the dependence of the PV current on the number \bar{N}_i of photons in a single-mode resonator is shown in Fig. 1(a), for the case of any mesoscopic conductor with fluctuating transmission matrix. For

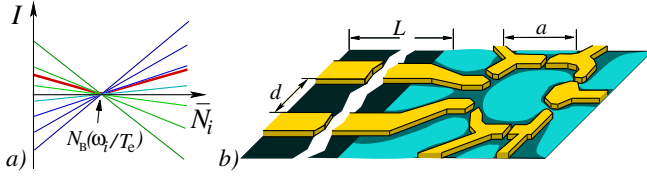


FIG. 1 (color online). (a) Schematic dependence of the PV current of a mesoscopic conductor on the average photon number \bar{N}_i in a single-mode resonator. Narrow lines represent the current magnitude of the current for various conductor realizations. The current vanishes for *all* realizations for $\bar{N}_i = N_B(\omega_i/T)$. The bold line is the rms value of the current over the ensemble. (b) A possible experimental setup for the observation of the quantum photovoltaic effect. Two gates are terminals of a high quality microwave line of length L , that form an EM resonator. To reduce dissipation, the substrate of the resonator contains 2DEG (brighter area) only in the vicinity of a quantum dot.

a particular realization of the conductor, the current is a linear function of \bar{N}_i and changes its direction at $\bar{N}_i = N_B(\omega_i/T)$; at large values of \bar{N}_i the dependence on \bar{N}_i will depart from linearity due to the suppression of the coherence time by electron—photon scattering. We note that the average value of the current with respect to realizations of the mesoscopic conductor is zero, since the parity violation of transmission is zero on average. In this case we characterize the magnitude of this current by its rms value averaged over the ensemble, shown in Fig. 1(a) by a bold line.

The generation of the photovoltaic current studied here is a common phenomenon for out-of-equilibrium mesoscopic systems, which function as “quantum ratchets”. Other similar phenomena are the Coulomb drag current [18] and the current in mesoscopic metal rings coupled to out-of-equilibrium electron [19] or phonon [20] reservoirs.

Model.—The signatures of the quantum behavior of the EM field can be observed in the PV current measurements for various mesoscopic systems, such as quantum point contacts [5], metal rings [12], metal wires or grains, and semiconductor quantum dots [6]. The main requirement is that the device has long coherence and inelastic relaxation times, so that electron interference in propagation through the device leads to strong energy dependence and intrinsic parity violation in transmission to the left and right lead. Any such mesoscopic device will show a PV current with the properties depicted in Fig. 1(a).

The specific case we will now treat in detail is the PV current through a semiconductor quantum dot with a few open channels placed at the terminal of an electromagnetic resonator; see Fig. 1(b). The quantum dot is similar to those used in charge pumping experiments [7,15]. The electromagnetic resonator consists of a microwave line of length L , characterized by a high quality factor and resonant frequencies $\omega_i = i\pi c_*/L$ [16], where c_* is the phase velocity of the EM wave in the resonator and $i = 1, 2, \dots$. The Hamiltonian of this system is

$$\mathcal{H} = \mathcal{H}_d + \mathcal{H}_f + \mathcal{H}_l + \mathcal{H}_{ld}, \quad (1)$$

where $\hat{\mathcal{H}}_d$ is the Hamiltonian of the electrons in the dot

$$\mathcal{H}_d = \sum_{n,m=1}^M \psi_n^\dagger \left[\hat{H} + \sum_i \hat{V}_i (a_i^\dagger + a_i) \right]_{nm} \psi_m. \quad (2)$$

Here ψ_n and a_i are the annihilation operators of electrons in the dot in state n ($n = 1, \dots, M$) and photons in mode i of the EM field, $M \times M$ Hermitian matrices \hat{H} and \hat{V}_i represent the stationary part of the electron Hamiltonian and the electron coupling to mode i of the EM field, respectively. $\hat{\mathcal{H}}_f$ describes the evolution of the electromagnetic field and can be written in terms of photon annihilation and creation operators a_i and a_i^\dagger

$$\hat{\mathcal{H}}_f = \sum_i \omega_i [a_i^\dagger a_i + 1/2], \quad (3)$$

where ω_i is the energy of photon excitations.

The Hamiltonian for electrons in the leads near the Fermi surface is

$$\hat{\mathcal{H}}_l = v_F \sum_{\alpha,k} k \psi_\alpha^\dagger(k) \psi_\alpha(k), \quad (4)$$

where $\psi_\alpha(k)$ is the annihilation operator of electrons in channel α of one of the leads. The continuous variable k denotes electron momenta in the leads, $v_F = (2\pi\nu)^{-1}$ is the Fermi velocity, and ν is the density of states per channel per spin at the Fermi surface. In this Letter we consider the case when the voltage bias across the dot is zero. The coupling of electron states in the dot to states in the leads can be written as

$$\hat{\mathcal{H}}_{ld} = \sum_{\alpha,n,k} (W_{n\alpha} \psi_\alpha^\dagger(k) \psi_n + \text{H.c.}). \quad (5)$$

Here α labels channels in the leads, with $1 \leq \alpha \leq N_l$ for the N_l channels in the left lead and with $N_l + 1 \leq \alpha \leq N_{\text{ch}}$ for the N_r channels in the right lead, $N_{\text{ch}} = N_l + N_r$. The coupling between electron states in the leads and in the dot is described by $N_{\text{ch}} \times M$ matrix \hat{W} .

Photovoltaic current.—We calculate the PV current that flows through a quantum dot at zero temperature and voltage biases. The interaction of electrons with the EM field results in the deviation of the electron distribution function $n_d(\varepsilon)$ in the dot from the Fermi distribution function $n_F(\varepsilon) = [1 + \exp(\varepsilon/T_e)]^{-1}$ of electrons in the leads at temperature T_e and in a finite electric current through the quantum dot. The direction and the magnitude of such current depend on the mesoscopic violation of the left-right symmetry of the dot, on the electron spectrum in the dot, and on the coupling strength of electrons to the EM field. The derivation of the expression for the current follows along the lines for the calculation of the current through open quantum dots coupled to classical external fields [6]. In the case of quantum fields, the field acquires the off-diagonal matrix elements in the Keldysh space, which can be easily taken into account within a bilinear response. As a result, we have

$$I = e \sum_i \sum_{\pm} \int J_i(\varepsilon, \pm \omega_i) R_i(\varepsilon, \pm \omega_i) d\varepsilon. \quad (6)$$

The kernel $J_i(\varepsilon, \omega)$ contains all the information about electron motion in the dot

$$\frac{J_i(\varepsilon, \omega)}{4\pi\nu} = \text{Tr}[\hat{W} \hat{\Lambda} \hat{W}^\dagger \hat{G}_r(\varepsilon) \hat{V}_i \text{Im}\{\hat{G}_r(\varepsilon - \omega)\} \hat{V}_i^\dagger \hat{G}_a(\varepsilon)] \quad (7)$$

and corresponds to the triangle vertex diagram for the Coulomb drag [18], written for the open dot geometry. Function $\hat{G}_r(\varepsilon)$ is defined for a given realization of \hat{H} by

$$\hat{G}_r(\varepsilon) = \frac{1}{\varepsilon - \hat{H} - i\pi\nu\hat{W}\hat{W}^\dagger}; \quad \hat{G}_a = [\hat{G}_r]^\dagger. \quad (8)$$

Here $\hat{\Lambda} = (N_r/N_{\text{ch}})\hat{\Lambda}_l - (N_l/N_{\text{ch}})\hat{\Lambda}_r$, where $[\hat{\Lambda}_l]_{\alpha\beta} = \delta_{\alpha\beta}$ for $1 \leq \alpha, \beta \leq N_l$, and $[\hat{\Lambda}_l]_{\alpha\beta} = 0$ otherwise; $\hat{\Lambda}_r = \hat{1} - \hat{\Lambda}_l$. Equation (6) takes into account spin degeneracy.

The function $R_i(\varepsilon, \omega_i)$ is a combination of the Fermi n_F and Bose N_B functions, and the photon occupation number $\bar{N}_i = \langle a_i^\dagger a_i \rangle$ for the i mode of the EM field:

$$R_i(\varepsilon, \omega) = 2[\bar{N}_i - N_B(\omega/T_e)][n_F(\varepsilon - \omega) - n_F(\varepsilon)]. \quad (9)$$

The contribution to the current I from mode i of the EM field is linear in the average number \bar{N}_i of photons with energy ω_i . If only one mode of electromagnetic field is coupled to electrons in the dot, the current I can be used to determine the average number of photons in this mode.

The structure of Eq. (9) can be understood from the following schematic argument. The distribution function in the dot $n_d(\varepsilon)$ is the solution of the kinetic equation

$$\frac{n_d(\varepsilon) - n_F(\varepsilon)}{\tau_{\text{esc}}} = \sum_i [\Gamma_i^{\text{ab}}(\varepsilon) - \Gamma_i^{\text{em}}(\varepsilon)]. \quad (10)$$

Here the left-hand side describes the relaxation of the distribution function $n_d(\varepsilon)$ due to electron escape to the leads with characteristic escape time τ_{esc} and the right-hand side represents the imbalance between the rates of absorption and emission of photons. These rates are determined by $n_d(\varepsilon)$ and by the average number of photons \bar{N}_i in mode i of the electromagnetic field:

$$\begin{aligned} \Gamma_i^{\text{ab}} &\propto \bar{N}_i n_d(\varepsilon) [1 - n_d(\varepsilon + \omega_i)], \\ \Gamma_i^{\text{em}} &\propto [\bar{N}_i + 1] n_d(\varepsilon + \omega_i) [1 - n_d(\varepsilon)]. \end{aligned} \quad (11)$$

Equations (10) and (11) determine the distribution function in the dot $n_d(\varepsilon)$. To the lowest order in electron coupling to the EM field, we can substitute $n_d(\varepsilon) = n_F(\varepsilon)$ in Eq. (11) and obtain $[\Gamma_i^{\text{ab}}(\varepsilon) - \Gamma_i^{\text{em}}(\varepsilon)] \propto R_i(\varepsilon, \omega_i)$. A similar expression for the electric current was also obtained in [20] for electrons coupled to out-of-equilibrium phonons.

When the thermal state of the EM field at temperature T_f is equal to electron temperature T_e , $\bar{N}_i = N_B(\omega_i/T_e)$, the solution of Eq. (10) is $n_d(\varepsilon) \equiv n_F(\varepsilon)$ and the PV current vanishes, as expected for a system in full thermodynamic equilibrium. Note, however, that the PV current does *not vanish* when there are no photons in the cavity, $\bar{N}_i = 0$. In this case the current is driven by electron relaxation through spontaneous emission of photons to the unoccupied modes of the EM field.

Below we consider the case when the electromagnetic field is in a thermal state at temperature T_f and $\bar{N}_i = N_B(\omega_i/T_f)$. Function $R_i(\varepsilon, \omega)$ contains $N_B(\omega_i/T_f) - N_B(\omega_i/T_e)$ and vanishes identically for $T_f = T_e$. For small deviations of T_f from T_e , the current I is linear in the temperatures difference: $I = B(T_f - T_e)$, where the EM field thermopower coefficient B is

$$B = e \sum_i \int [J_i(\varepsilon, \omega_i) r(\varepsilon, \omega_i) - J_i(\varepsilon, -\omega_i) r(\varepsilon, -\omega_i)] d\varepsilon, \quad (12)$$

$$r(\varepsilon, \omega) = \frac{\omega/[4T_e^2 \sinh(\omega/2T_e)]}{\cosh(\varepsilon/2T_e) \cosh[(\varepsilon - \omega)/2T_e]}.$$

Equation (12) determines the value of the EM field thermopower coefficient B for a particular realization of the Hamiltonian \hat{H} of the quantum dot. Theoretical and experimental work [21,22] has shown that lateral quantum dots are well described by a random-matrix (RM) model due to the chaotic motion of electrons. Therefore the theory of such systems has focused on calculating averages of relevant statistical quantities over an appropriate RM ensemble. Below we calculate the statistical properties of B with respect to a RM ensemble of \hat{H} .

Mesoscopic fluctuations of the current.—We calculate mesoscopic fluctuations of thermopower coefficient B with respect to realizations of the $M \times M$ matrix \hat{H} from a Gaussian ensemble of Hermitian matrices with $M \rightarrow \infty$, characterized by the mean level spacing δ_1 : $\langle H_{nm} H_{nm}^* \rangle = (M\delta_1^2/\pi^2) \delta_{nn'} \delta_{mm'}$ for a unitary ensemble (The result is the same for unitary and orthogonal ensembles). The quantity of interest is the dimensionless quantity representing the ensemble average product of interaction matrices \hat{V}_i :

$$\Gamma_{ij} = \frac{2\pi^2}{N_{\text{ch}}} \frac{\langle \text{Tr}\{\hat{V}_i \hat{V}_j\} \rangle_{\text{ens}}}{(M\delta_1)^2}. \quad (13)$$

The coupling constants between electron states in the dot and in the leads are $W_{n\alpha} = \delta_{n\alpha} \sqrt{M\delta_1/\pi^2} \nu$ and result in the following value of the electron escape rate from the dot: $\gamma_{\text{esc}} = 1/\tau_{\text{esc}} = N_{\text{ch}} \delta_1/2\pi$. Note that γ_{esc} plays the role of the Thouless energy of diffusive systems, it sets the scale of variation of the transmission with electron energy.

The ensemble average value of B is zero. The variance of the PV current can be calculated by diagrammatic RM technique [23] and is given by

$$\text{var } B = e^2 \frac{N_l N_r}{N_{\text{ch}}^2} \sum_{ij} \frac{\Gamma_{ii} \Gamma_{jj}}{\gamma_{\text{esc}}^2} \mathcal{K}_{ij}, \quad (14)$$

where the kernel \mathcal{K}_{ij} is

$$\begin{aligned} \mathcal{K}_{ij} &= K_{\omega_i, \omega_j} - K_{-\omega_i, \omega_j} - K_{\omega_i, -\omega_j} + K_{-\omega_i, -\omega_j}; \\ K_{\omega_i, \omega_j} &= 4\gamma_{\text{esc}}^2 \int \left[3 + \frac{2[\Gamma_{ij}^2/(\Gamma_{ii}\Gamma_{jj})]\gamma_{\text{esc}}^2}{\gamma_{\text{esc}}^2 + (\varepsilon - \varepsilon' + \omega_j - \omega_i)^2} \right] \\ &\quad \times \frac{r(\varepsilon, \omega_i) r(\varepsilon, \omega_j)}{\gamma_{\text{esc}}^2 + (\varepsilon - \varepsilon')^2} d\varepsilon d\varepsilon'. \end{aligned} \quad (15)$$

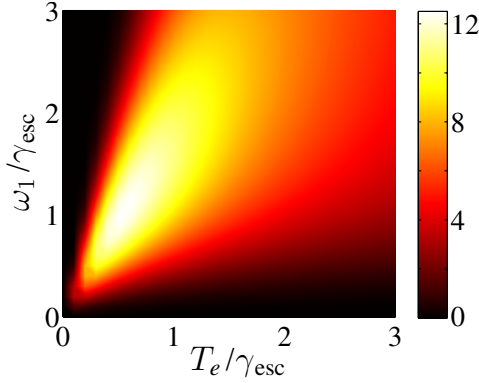


FIG. 2 (color online). False color plot of the kernel \mathcal{K} determining the rms PV current as a function of its arguments, the cavity mode frequency, ω_1 , and the electron temperature, T_e , in units of the electron escape rate γ_{esc} from the dot.

To analyze the properties of the variance of the thermoelectric coefficient B , we consider the case when only one mode $i = 1$ of the electromagnetic field is coupled to electrons in the quantum dot. The contour plot of $\mathcal{K}_{11} = \mathcal{K}(\omega_1/\gamma_{\text{esc}}, T_e/\gamma_{\text{esc}})$ is shown in Fig. 2.

In the low frequency limit of $\omega_1 \ll \gamma_{\text{esc}}$, the power law $\mathcal{K}(\omega_1/\gamma_{\text{esc}}, T_e/\gamma_{\text{esc}}) \sim \omega_1^4$ is similar to the dependence of the variance of the PV current induced by a single-parameter classical perturbation [6]. At low temperature $T_e \ll \omega_1$, the number of photons and electron-hole pairs is exponentially suppressed and $\mathcal{K} \propto \exp(-\omega_1/T_e)$. At high temperature $T_e \gg \gamma_{\text{esc}}$, the contribution to the thermoelectric coefficient comes from electron states within thermal energies and becomes self-averaged. As a result of such self-averaging, the variance of B decreases as $\mathcal{K} \sim 1/T_e$ as T_e increases. To summarize, $\mathcal{K}(\omega_1/\gamma_{\text{esc}}, T_e/\gamma_{\text{esc}})$ has a maximum at $T \propto \omega_1$ at fixed ω_1 , see Fig. 2. The global maximum of $\mathcal{K}(\omega_1/\gamma_{\text{esc}}, T_e/\gamma_{\text{esc}})$ is $\mathcal{K}_{\text{max}} \approx 12.5$ at $\omega_1 \approx 1.2\gamma_{\text{esc}}$ and $T_e \approx 0.6\gamma_{\text{esc}}$. Thus, the largest effect will be observed when $T_e \sim \omega_1 \sim \gamma_{\text{esc}}$.

Conclusions.—We discuss experimentally achievable values of the system parameters (restoring \hbar and k_B in the equations below). In experiments [16] $\omega_1/2\pi \sim 10$ GHz ($\hbar\omega_1/k_B \approx 0.5$ K) and $T_f \approx 30$ mK. The escape rate γ_{esc} for $N_{\text{ch}} \sim 1$ is comparable with $\delta_1/2\pi\hbar \approx 2.5$ GHz ($\delta_1/k_B \approx 0.12$ K) [7].

To estimate the rms value of the thermoelectric coefficient $B_{\text{rms}} = \sqrt{\text{var}B}$, we write $B_{\text{rms}} \sim e\Gamma_{11}(k_B/\hbar)$, see Eq. (14), where Γ_{11} is defined by Eq. (13) and can be expressed in terms of the magnitude of zero-point electric field E_1 of the lowest frequency mode $i = 1$ of the EM resonator as $\Gamma_{11} \approx e^2 E_1^2 a^2 \tau_i \tau_{\text{esc}}/\hbar^2$ [23], where a is the diameter of the dot, see Fig. 1, and $\tau_i = a/v_F$. The field E_1 can be estimated from $(E_1^2/4\pi)d^2L \sim \hbar\omega_1/2$, where $L = \pi c_*/\omega_1$ is the resonator length, and gives $B_{\text{rms}} \sim e\alpha_*(k_B/\hbar)(\omega_1^2 \tau_i \tau_{\text{esc}})$, where $\alpha_* = e^2/\hbar c_*$ and $a \sim d$. Compared to the usual thermopower due to the temperature

difference between the leads [24], the EM thermopower at $T_e \approx \hbar\gamma_{\text{esc}}/k_B$ is suppressed by factor $\alpha_*\tau_i\gamma_{\text{esc}} \ll 1$. At $\omega_1/2\pi = 10$ GHz and $\tau_i = 4 \times 10^{-12}$ s, we have $B_{\text{rms}} \sim 35$ pA/K, and for $|T_f - T_e| \approx 0.1$ K the current \sim pA is in the observable range.

We thank I. Aleiner, V. Manucharyan, and C. Marcus for discussions. This work was supported by the W.M. Keck Foundation and by NSF ITR No. DMR-0325580 and NSF Materials Theory Grant No. DMR-0408638.

*Present address: Department of Physics, University of Wisconsin, Madison, WI 53706, USA.

- [1] F. Giazotto *et al.*, Rev. Mod. Phys. **78**, 217 (2006).
- [2] B. Altshuler *et al.*, in *Sov. Sci. Rev. A:Phys.* (Harwood Academic, Chur, Switzerland, 1987), Vol. 9, p. 223.
- [3] B.L. Altshuler *et al.*, *Quantum Theory of Solids* (Mir, Moscow, 1982).
- [4] V.I. Falko, Zh. Eksp. Teor. Fiz. **92**, 704 (1987).
- [5] V.I. Fal'ko and D.E. Khmel'nitskii, Sov. Phys. JETP **68**, 186 (1989).
- [6] M.G. Vavilov, V. Ambegaokar, and I.L. Aleiner, Phys. Rev. B **63**, 195313 (2001).
- [7] L. DiCarlo, C.M. Marcus, and J.S. Harris, Phys. Rev. Lett. **91**, 246804 (2003).
- [8] M.G. Vavilov, L. DiCarlo, and C.M. Marcus, Phys. Rev. B **71**, 241309(R) (2005).
- [9] F. Zhou, B. Spivak, and B. Altshuler, Phys. Rev. Lett. **82**, 608 (1999).
- [10] P.W. Brouwer, Phys. Rev. B **58**, R10 135 (1998).
- [11] M.L. Polianski and P.W. Brouwer, J. Phys. A **36**, 3215 (2003).
- [12] V.E. Kravtsov and V.I. Yudson, Phys. Rev. Lett. **70**, 210 (1993).
- [13] A.A. Bykov, G.M. Gusev, and Z.D. Kvon, Sov. Phys. JETP **70**, 742 (1990).
- [14] H. Linke *et al.*, Europhys. Lett. **44**, 341 (1998).
- [15] M. Switkes *et al.*, Science **283**, 1905 (1999).
- [16] A. Wallraff *et al.*, Nature (London) **431**, 162 (2004).
- [17] T.A. Shutenko, I.L. Aleiner, and B.L. Altshuler, Phys. Rev. B **61**, 10 366 (2000).
- [18] B.N. Narozhny and I.L. Aleiner, Phys. Rev. Lett. **84**, 5383 (2000); the diagrammatic formalism for the Coulomb drag can be found in A. Kamenev and Y. Oreg, Phys. Rev. B **52**, 7516 (1995).
- [19] O.L. Chalaev and V.E. Kravtsov, Phys. Rev. Lett. **89**, 176601 (2002).
- [20] V.I. Yudson and V.E. Kravtsov, Phys. Rev. B **67**, 155310 (2003).
- [21] A. Altland, C.R. Offer, and B.D. Simons, in *In proceedings of the 1997 Summer School "Disordered Systems and Quantum Chaos"*, edited by I.V. Lerner (Kluwer, New York, 1999).
- [22] I.H. Chan *et al.*, Phys. Rev. Lett. **74**, 3876 (1995).
- [23] M.G. Vavilov, J. Phys. A **38**, 10 587 (2005).
- [24] M.G. Vavilov and A.D. Stone, Phys. Rev. B **72**, 205107 (2005).